Sb-NMR/NQR studies of heavy fermion system YbRhSb

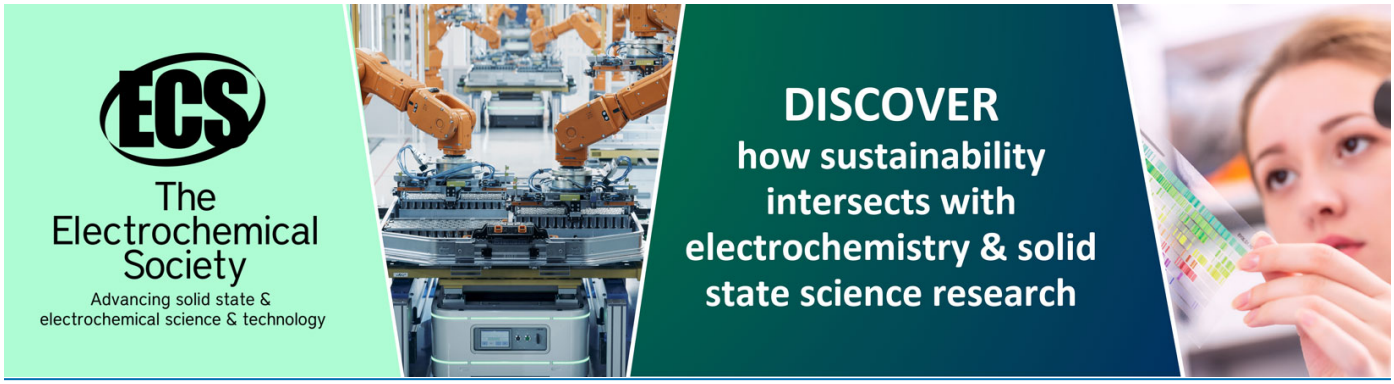

IOP Conf. Series: Journal of Physics: Conf. Series **807** (2017) 012014 doi:10.1088/1742-6596/807/1/012014

Sb-NMR/NQR studies of heavy fermion system YbRhSb

Yasuki Kishimoto[1], Yosiki Awai[1], Hisashi Kotegawa[1], Hideki Tou[1*], Yuji Muro[2], Koji Nakamura[3], Masafumi Sera[3], and Toshiro Takabatake[3]

[1] *Department of Physics, Graduate School of Science, Kobe University, Kobe 657-8501, Japan*
[2] *Department of Intelligent Systems Design Engineering, Faculty of Engineering, Toyama Prefectural University, Imizu, Toyama 939-0398, Japan*
[3] *Department of Quantum Matters, AdSM, Hiroshima University, Higashi-Hiroshima, Hiroshima, Japan*

E-mail: *:tou@crystal.kobe-u.ac.jp

Abstract. We report a study of ^{121}Sb nuclear magnetic resonance (NMR) and nuclear quadrupole resonance (NQR) in a Yb-based heavy fermion system YbRhSb using a single crystal. Sharp ^{121}Sb-NMR lines were observed for each crystal axis for $B\|a, b, c$. From comparison with observed Sb-NMR spectra and numerical simulations, electric field gradient (EFG) parameters and Knight shift parameters are obtained at 10 K. The obtained quadrupole frequency, asymmetry parameter, isotropic Knight shift and anisotropic principal values of Knight shift tensors are $\nu_Q = 18.8$ MHz, $\eta = 0.2$, $K_{iso} \approx 0.6$ %, and $(K^x_{\rm ax}, K^y_{\rm ax}, K^z_{\rm ax}) \approx (-3.5, 4.1, -0.6)$ %, respectively. We also succeeded in observing ^{121}Sb-NQR signals at around 19.5 and 37 MHz, which are reproduced by the nuclear quadrupole Hamiltonian with $\nu_Q = 18.8$ MHz and $\eta = 0.2$. We mention the relation between the anisotropy of the Knight shift and magnetic susceptibility. Our NMR/NQR results suggest that the weak ferromagnetism in YbRhSb is ascribed to a canted antiferromagnetic state.

1. Introduction

RTX type compounds (R = Ce, Yb, U; T = Co, Ni, Rh, X =Sn, Sb, Ge) with the orthorhombic ε-TiNiSi-type structure have been attracted attention because these compounds show various exotic ground states. For example, CeNiSn is well known as a Kondo semiconductor.[1] The isostructural U-based counterpart UCoGe shows coexistence between ferromagnetic state and superconductivity.[2]

Among them, Yb-based compounds with ε-TiNiSi-type structure shows unusual ferromagnetic properties. YbNiSn undergoes a ferromagnetic transition at $T_C \approx 5.6$ K with the ordered moment $\mu_s \approx 0.85\mu_B$/Yb.[3, 4] An electronic specific-heat coefficient is $\gamma \approx 300$ mJ/mol K below T_C, suggesting YbNiSn is classified into a class of heavy fermion ferromagnets.[5]

YbRhSb also reveals a ferromagnetic transition at $T_C \approx 2.7$ K.[6] The spontaneous moment is, however, unusually small of $\approx 3.0\times10^{-3}$ μ_B/Yb for the applied field (B) parallel to the crystal b-axis. A metamagnetic transition was observed at around 2 T and the magnetization reaches $1.4\mu_B$/Yb for $B\|a$-axis at 15 T. In addition, T_C decreases with the increase of magnetic field, differently from the behavior of typical ferromagnets. Moreover, a large electronic specific-heat

coefficient is $\gamma \approx$370 mJ/mol K^2 in the ferromagnetic ordered state. However, it is strange that the largest spontaneous magnetization appears for the field direction parallel to the b axis below T_C, nevertheless the magnetic easy axis is the a axis in the paramagnetic state. These behaviors suggest that the weak ferromagnetism of YbRhSb is ascribed to a canted antiferromagnetic structure.[6]

In order to clarify microscopically the unusual weak ferromagnetic state, we carried out ^{121}Sb-nuclear magnetic resonance (NMR) and nuclear quadrupole resonance measurements on YbRhSb. Here we determine the ^{121}Sb-NMR/NQR parameters.

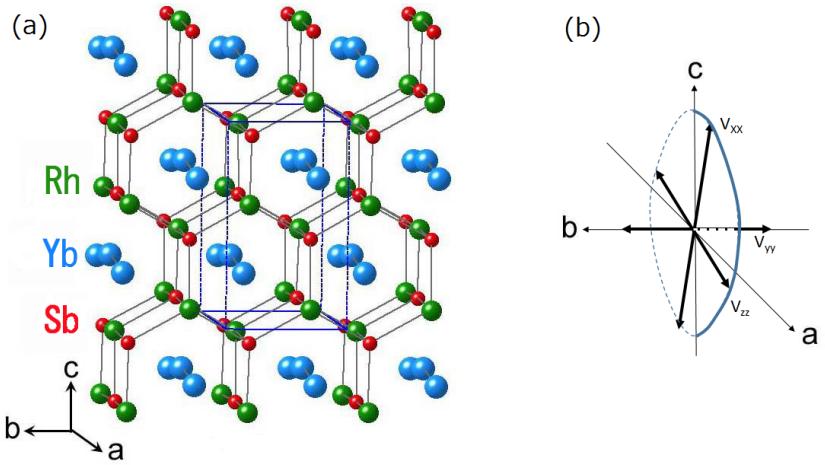

Figure 1. (a) Schematic crystal structure of YbRhSb. Unit cell is drown by blue dashed line. (b) Schematic figure of the principal axes of EFG tensors at Sb site.

2. Experimental

Single-crystalline samples of YbRhSb were grown by using the Bridgeman method. Stoichiometric amounts of the elements were sealed in a molybdenum crucible by arc welding under a purified argon atmosphere. The crucible was heated up to 1600 °C in a vacuum by using a tungsten mesh heater and slowly cooled. [6]

The powder x-ray-diffraction pattern showed that YbRhSb crystallizes with the orthorhombic ε-TiNiSi-type structure and the space group is $No.62, Pnma$.[6] The lattice constants is a = 7.004 Å, b = 4.492 Å, and c = 7.731 Å. The electron-probe microanalysis (EPMA) revealed the presence of an impurity phase $YbSb_2$ of less than 0.1% of the stoichiometric host phase. The single-crystal nature of the sample was also confirmed by the x-ray Laue diffraction method. The electrical resistivity, dc magnetic susceptibility measurements and specific heat measurements evidence a magnetic phase transition at 2.7 K.[6] The single-crystal sample was used for the NMR measurements, where the dimensions of the cuboidal sample were $L(a\text{-axis}) \times W(b) \times H(c) \approx 3 \times 3 \times 2$ mm^3.

^{121}Sb ($I = 5/2$, $^{121}\gamma_n/2\pi$ = 10.189 MHz/10 kOe, and $^{121}Q = -0.597 \times 10^{-28}$ m^2) NMR measurements for the single-crystal sample was carried out by using a conventional pulsed spectrometer. The ^{121}Sb nuclear magnetic resonance (NMR) spectrum was obtained by tracing the spin-echo intensity as a function of the magnetic field. The ^{121}Sb nuclear quadrupole resonance (NQR) spectrum was obtained by tracing the spin-echo intensity as a function of the frequency. A part of the obtained single-crystal sample was crushed into powder form with smaller grain size than the skin depth for NMR measurements to gain a signal to noise ratio at high temperatures.

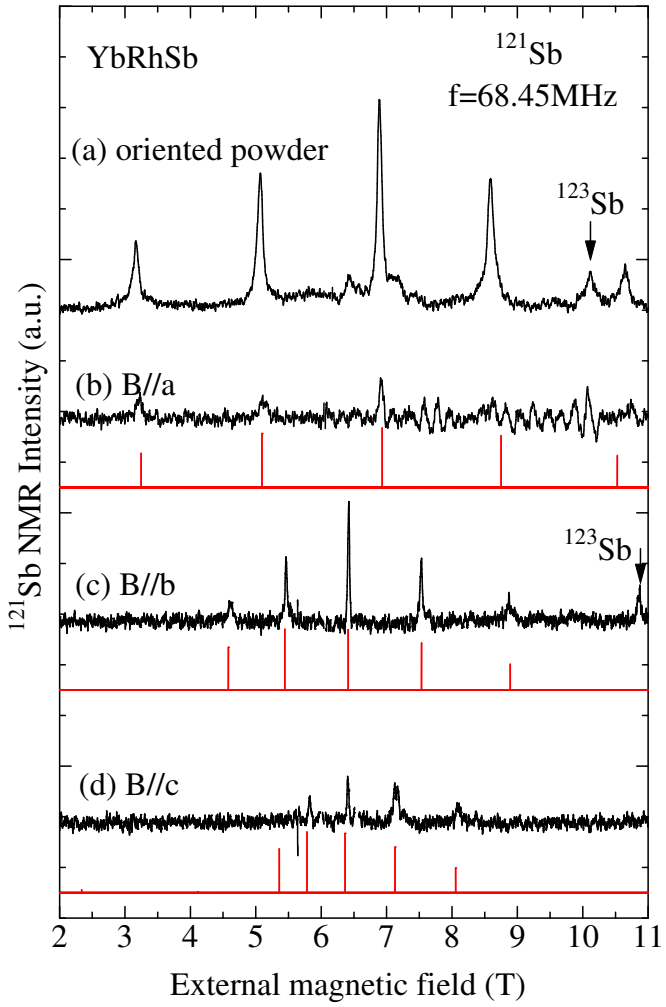

Figure 2. ^{121}Sb-NMR spectra for (a) oriented-powder, (b) $B\|a$, (c) $B\|b$, (d) $B\|c$-axes. Red solid lines are results of simulations for each field angle (see text).

3. Results and Discussions

Figure 2 shows the entire ^{121}Sb-NMR spectra for $B\|a, b$, and c directions observed at the fixed frequency $f = 68.45\,\mathrm{MHz}$ at $T = 10\,\mathrm{K}$. ^{121}Sb nucleus has the nuclear spin $I = 5/2$, then the ^{121}Sb-NMR line splits into five lines. In order to reproduce the observed NMR spectra, the resonance fields were calculated by an exact-diagonalization method for the 6×6 nuclear spin Hamiltonian matrix of ^{121}Sb nucleus. The Hamiltonian is written as,

$$\begin{aligned}\mathcal{H} &= -\gamma_{\mathrm{n}}\hbar I_z H_0 - \gamma_{\mathrm{n}}\hbar I_z H_0 K_{\mathrm{iso}} - \gamma_{\mathrm{n}}\hbar (K^z_{\mathrm{an}} I_z H_z + K^x_{\mathrm{an}} I_x H_x + K^y_{\mathrm{an}} I_y H_y) \\ &+\frac{1}{6}h\nu_{\mathrm{Q}}\left[\left(3\cos^2\theta - \eta\cos 2\phi \sin^2\theta\right) I_z^2 + \frac{1}{4}\left\{3\sin^2\theta - \eta\cos 2\phi\left(1+\cos^2\theta\right)\right\}\left(I_+^2 + I_-^2\right)\right. \\ &+\frac{1}{4}\sin^2\theta\,(3+\eta\cos 2\phi)\,(I_+ I_- + I_- I_+) - I\,(I+1)\end{aligned}$$

$$-i\left(\frac{1}{2}\eta\sin 2\phi\cos\theta\left(I_+^2-I_-^2\right)+\frac{1}{4}\sin 2\theta\left(3+\eta\cos 2\phi\right)\left\{\left(I_+-I_-\right)I_z+I_z\left(I_+-I_-\right)\right\}\right)\Bigg]. \tag{1}$$

The first term is the Zeeman interaction, the second term is the hyperfine interaction described by the isotropic part of the Knight shift, $K_{\rm iso}$, and the principal values of anisotropic Knight shift tensors, ($K_{\rm an}^x$, $K_{\rm an}^y$, $K_{\rm an}^z$), where the shift tensors fulfills the relation of $K_{\rm an}^x+K_{\rm an}^y+K_{\rm an}^z=0$. The third one describes the nuclear quadrupole interaction. Here, h is the Planck constant and $\hbar\equiv h/2\pi$. $\nu_{\rm Q}$ is the NQR frequency and is defined by $\nu_{\rm Q}\equiv 3eQV_{zz}/2hI(2I-1)$. η is the asymmetry parameter and is defined by $\eta\equiv\left(V_{xx}-V_{yy}\right)/V_{zz}$. V_{xx}, V_{yy}, and V_{zz} are the principal values of the electric field gradient (EFG) where $V_{zz}\geq V_{xx}\geq V_{yy}$. θ is the polar angle of the field direction with respect to V_{zz}, and ϕ is the azimuth angle of the field direction with respect to V_{xx}. For simplicity, we assumed that the principal axes of the EFG tensor coincide with those the Knight shift tensors.

In fact, the second order perturbation theory for the above nuclear Hamiltonian assuming $\nu_L\gg\nu_Q$, where $\nu_L=\frac{\gamma}{2\pi}H_0$, yields following equation for the transition frequency between mth and $m-1$th level:

$$\begin{aligned}
h\nu_{m\leftrightarrow m-1} &= h(1+K_{iso})\nu_L+\frac{1}{2}h\left[\nu_Q\left(\frac{1}{2}-m\right)-K_{\rm an}^z\nu_L\right]\left(3\cos^2\theta-1\right)\\
&\quad-\frac{1}{2}h\left[\nu_Q\eta\left(\frac{1}{2}-m\right)+\left(K_{\rm an}^y-K_{\rm an}^x\right)\nu_L\right]\cos 2\phi\sin^2\theta\\
&\quad+\frac{\nu_Q^2}{12(1+K_{iso})\nu_L}\left[\frac{3}{2}\sin^2\theta\left\{(A+B)\cos^2\theta-B\right\}\right.\\
&\qquad\left.+\eta\cos 2\phi\sin^2\theta\left\{(A+B)\cos^2\theta+B\right\}\right]\\
&\quad+\frac{\nu_Q^2}{72(1+K_{iso})\nu_L}\eta^2\left[A-(A+4B)\cos^2\theta-(A+B)\cos^2 2\phi(1-\cos^2\theta)^2\right],
\end{aligned} \tag{2}$$

where $A=24m(m-1)-4I(I+1)+9$ and $B=\frac{1}{4}\left\{6m(m-1)-2I(I+1)+3\right\}$. Thus, the resonance frequency depends on H_0, ν_Q, η, $K_{\rm iso}$, $K_{\rm an}^i(i=x,y,z)$, and field angle θ, ϕ with respect to the EFG principal axes. Then, the quadrupole frequency ν_Q should be slightly different from the peak positions of the observed NQR signals, as described later.

Red solid lines in Fig. 2 are the results of the simulations for each field direction with respect to the crystal axes. In order to reproduce the obtained NMR spectra, we obtained NMR/NQR parameters as follows: Isotropic and anisotropic NMR Knight shifts are $K_{iso}\approx 0.6$ % and $(K_{\rm an}^x,K_{\rm an}^y,K_{\rm an}^z)\approx(-3.5,4.1,-0.6)$ %, respectively. NQR quadrupole frequency and asymmetry parameter are $\nu_Q=18.8$ MHz, $\eta=0.2$. Here, the angle-sets (θ,ϕ) are obtained to be $(7^\circ,0^\circ)$ for $B\|a$, $(90^\circ,7^\circ)$ for $B\|b$, and $(97^\circ,0^\circ)$ for $B\|c$. Thus we found that V_{yy} lies along b-axis, whereas respective V_{zz} and V_{xx} rotate from the a- and c-axes by $\sim 7^\circ$, as shown in the fig. 1(b). The reason why the principal EFG tensors do not coincide with the crystal axes is attributed to the lower symmetry of the crystal structure. In fact, the local symmetry at Sb site at Wycoff position 4c is .m., then only a mirror plane exists perpendicular to the b-axis. Thus, Sb 4c site does not have a local spatial symmetry.

We found from the anisotropic Knight shift that the maximum principal value of the Knight shift tensors is $K_{\rm an}^y$ for $B\|b$ axis, being incompatible with the susceptibility that the magnetic easy axis is a axis. This contradiction may be a possible origin for the weak ferromagnetism, i.e., a canted antiferromagnetic state, in YbRhSb. Furthermore, we should notice that the Wycoff position of the Yb site is same as that of the Sb site. That is, the local spatial symmetry

is broken at Yb site. In this case, a Dzyaloshinsky-Moriya type antisymmetric spin-orbit interaction[7] works and the alignment of the Yb magnetic moment might be forced to cant from the crystal axis. In fact, Dzyaloshinsky vector orients perpendicular to the *ac* plane (along *b* axis). This direction is consistent with the maximum principal direction of the Knight shift tensors. Therefore, we expect that the weak ferromagnetism in YbRhSb is arising from the lower symmetries of the Sb and Yb site. In any case, to check this scenario, measurements of the temperature dependences of both zero-field NMR and Knight shift are needed.

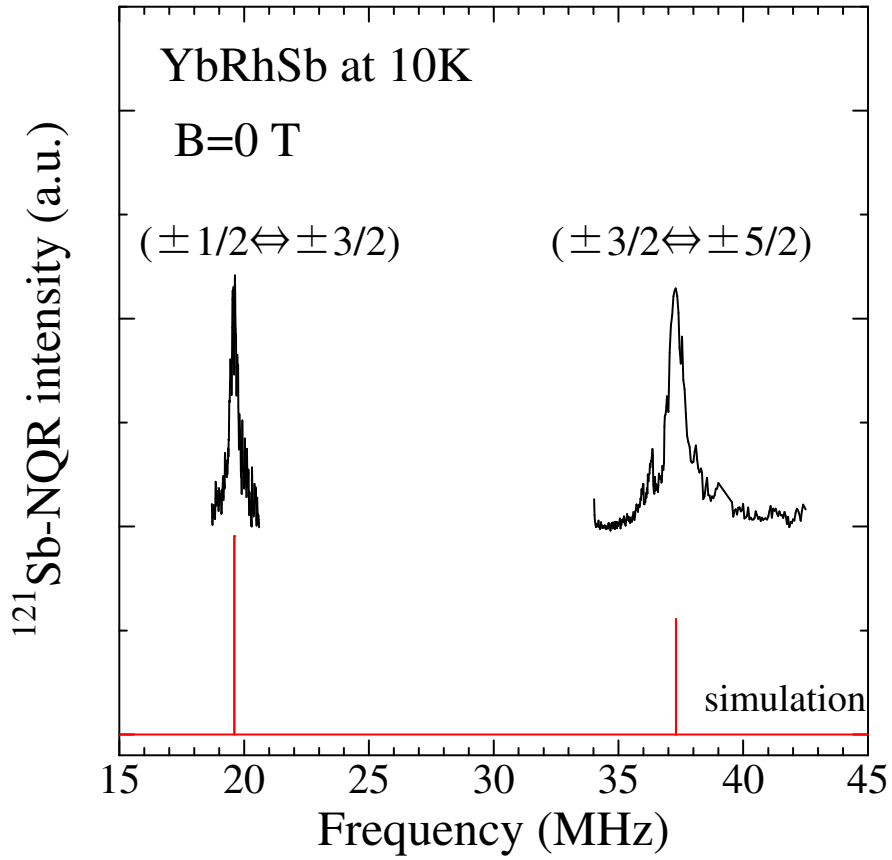

Figure 3. ^{121}Sb-NQR spectra of YbRhSb measured at 10 K. Respective resonance peaks at aroud ≈19.5 MHz and ≈37 MHz roughly correspond to the $(\pm\frac{1}{2} \leftrightarrow \pm\frac{1}{2})$ transition and $(\pm\frac{3}{2} \leftrightarrow \pm\frac{5}{2})$ transition.

We have succeeded in finding ^{121}Sb-NQR signals by using the NQR parameters. Figure 3 shows ^{121}Sb-NQR spectrum measured at 10 K. Red solid line is the result of the simulation with EFG parameters of $\nu_Q = 18.8$ MHz and $\eta = 0.2$. The good agreement between the experimental and simulation confirms that the obtained EFG parameters are valid.

4. Conclusions

We observed ^{121}Sb-NMR/NQR signals of a single crystal YbRhSb and determined ^{121}Sb NMR/NQR parameters. Notably, we succeeded in observing the Sb-NMR and NQR signals

and determining EFG parameters, isotropic Knight shift and anisotropic Knight shift tensors at Sb site for the first time. Our NMR/NQR results suggest that the weak ferromagnetism in YbRhSb is ascribed to a canted antiferromagnetic state. The present result allows us to explore the origin of the weak ferromagnetism in YbRhSb by measuring temperature and field dependences of ^{121}Sb Knight shift and nuclear spin-lattice relaxation rate $^{121}(1/T_1)$.

5. Acknowledgments

This work has been supported by JSPS KAKENHI Grant Numbers 15H05885, (J-Physics), 26400359, and 15H05745, and partly supported by JSPS KAKENHI Grant Numbers, and 15H03689, 15K05882, and 15K21732.

References

[1] Takabatake T, Teshima F, Fujii H, Nishigori S, Suzuki T, Fujita T, Yamaguchi Y, Sakurai J, and Jaccard D, 1990 *Phys Rev. B* **41**, 9607.
[2] Aoki D, Huxley A, Ressouche E, Braithwaite D, Flouquet J, Brison J.P, Lhotel E, and Paulsen C, 2001 *Nature London* **413**, 613 .
[3] Bonville P, Bellot P, Hodges J.A., Imbert P, Jehanno G, Le Bras G, Hammann J, Leylekian L, Chevrier G, Thuery P, DOnofrio L, Hamzic A, and Barthelemy A,1992 *Physica B* **182**, 105.
[4] Kasaya M, Tani T, Kawate K, Mizushima T, Isikawa Y, and Sato K, 1991 *J. Phys. Soc. Jpn.* **60**, 3145.
[5] Drescher K, Abd-Elmeguid M.M, Micklitz H, and Sanchez J.P, 1996 *Phys. Rev. Lett.* **77**, 3228.
[6] Muro Y, Haizaki Y, Kim M.S., Umeo K, Tou H, Sera M, and Takabatake T, 2004 *Phys. Rev. B* **69**, 020401(R).
[7] Moriya T, in Magnetism I, edited by G.T. Rado and H. Suhl (*Academic*, New York, 1963) p. 85.